Rev.Adv.Mater.Sci. 18(2008) 66-70

GLASS-FORMATION AND HARDNESS OF Mg-BASED MULTICOMPONENT ALLOYS

Paola Rizzi, Marta Satta and Marcello Baricco

Dipartimento di Chimica IFM, Centre of Excellence NIS, Università di Torino, V.Giuria 9, 10125 Torino, Italy

Received: March 29, 2008

Abstract. Multicomponent Mg-based alloys were solidified by melt spinning and by copper mould casting, obtaining ribbons and cone shaped samples with maximum diameter of 4 mm. Fully amorphous samples were obtained for $Mg_{60}Ni_9Cu_9Zn_5Y_6Ag_5Gd_6$ ingot up to the maximum diameter, but crystals embedded in an amorphous matrix have been found for $Mg_{51}Ni_{11}Cu_{13}Zn_4Y_5Ag_7Gd_9$ when cone samples are produced. Therefore, a reduction of the Mg content in the alloy produces a decrease in the GFA. The stability of the amorphous phase and the glass transition temperature were determined by calorimetric measurements. Vickers hardness tests were performed on as cast amorphous samples.

1. INTRODUCTION

In metallic materials with a glassy structure, properties different from the correspondent crystalline materials are observed, due to the structural nature of the amorphous phase. In particular, bulk metallic glasses (BMG), characterised by a high glass forming ability (GFA), show peculiar mechanical properties, such as high modulus of elasticity and high strength [1-3]. The combination of large thickness (i.e. of high GFA) and good mechanical properties are essential for possible applications of BMG as structural materials.

Among a large number of amorphous alloys, Mg-based alloys are interesting because of their high strength and low weight. Ternary systems with general composition Mg-TM-RE (with TM = transition metals such as Cu, Ni; RE = Y and rare earth elements such as Gd, Nd) show wide composition ranges in which amorphous bulk materials can be obtained by copper mould casting [4-6]. $Mg_{65}Cu_{25}Y_{10}$ alloy exhibit high GFA and can be obtained as amorphous phase with a diameter up to 4 mm [7]. The substitution of Y with Gd causes an improvement of GFA: $Mg_{65}Cu_{25}Gd_{10}$ BMG was produced with a maximum diameter of 8 mm by copper mold casting in air atmosphere [8]. A significant improvement in GFA was reported for multicomponent alloys [9,10]. For instance, $Mg_{65}Cu_{7.5}Ni_{7.5}Y_{10}Zn_5Ag_5$ BMG was produced with a diameter of 9 mm [11] and $Mg_{65}Cu_{7.5}Ni_{7.5}Y_5Gd_5Zn_5Ag_5$ alloy was obtained as an amorphous phase up to a diameter of 14 mm by Cu-mould casting in air atmosphere [12].

Goal of this work is to understand the influence of the Mg content on the GFA and microhardness of multicomponent alloys containing Ni, Cu, Zn, Y, Ag and Gd. A reduction of the Mg content was performed with respect to the $Mg_{65}Ni_{7.5}Cu_{7.5}Zn_5Y_5Ag_5Gd_5$ alloy [12], obtaining two master alloys ($Mg_{51}Ni_{11}Cu_{13}Zn_4Y_5Ag_7Gd_9$ and $Mg_{60}Ni_9Cu_9Zn_5Y_6Ag_5Gd_6$), named, in the following, Mg51 and Mg60, respectively. From master alloys, both ribbons and BMG were produced, in order to determine the critical size for glass formation. Hardness was also investigated in order to estimate the mechanical properties.

Corresponding author: Paola Rizzi, e-mail paola.rizzi@unito.it

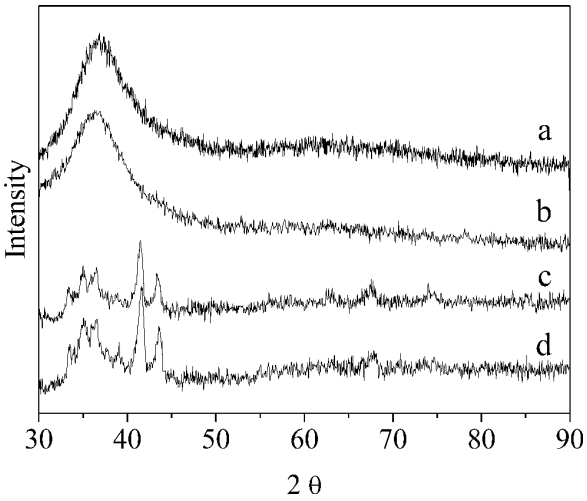

Fig. 1. XRD patterns of: (a) Mg51 as quenched ribbon; (b) Mg60 cone slices of 4 mm diameter; (c) Mg51 cone slices of 2 mm diameter; (d) Mg51 cone slices of 4 mm diameter.

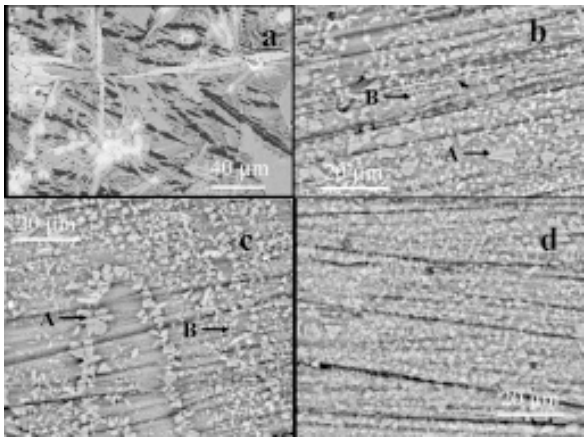

Fig. 2. SEM image (backscattered electrons) of Mg51 alloy: (a) master alloy; (b) cone slices of 4 mm diameter; (c) cone slices of 3 mm diameter; (d) cone slices of 2 mm diameter.

2. EXPERIMENTAL

The (Cu-Ni)-(Gd-Y)-Ag master alloys were prepared by arc melting pure elements. The ingot was then remelted in a BN crucible with Zn and Mg with an induction furnace under argon atmosphere. Ribbons with thickness of about 40 μm were prepared by melt spinning. Ingots were produced by casting the liquid alloys into a cone shaped copper mold with 30 mm in height, 4 mm in diameter at the top and 1 mm at the bottom. From cone-shaped samples, thin slices were cut in order to have samples with increasing diameter and, as a consequence, subject to decreasing quenching rates.

Structural informations were obtained performing X-Ray diffraction (XRD) analysis with Cu K_α radiation. The thermal stability of the amorphous phase was checked by differential scanning calorimetry (DSC) by using an heating rate of 40°C/min. Scanning Electron Microscopy (SEM) was used to study the microstructure of the master alloys and of the as quenched samples. The Vickers microhardness was determined, both on as quenched ribbons and bulk samples, by using 50 g load and 500 g load, respectively.

3. RESULTS AND DISCUSSION

$Mg_{51}Ni_{11}Cu_{13}Zn_4Y_5Ag_7Gd_9$

Mg51 ribbons were obtained fully amorphous by melt spinning as evidenced by the XRD pattern reported in Fig. 1 curve a. For the slices cut from bulk samples, XRD peaks due to crystalline phases were observed, beside a fraction of amorphous phase, which increase when the diameter of the slices is decreased, i.e. when the quenching rate is increased (Fig. 1, curves c and d). So, for this composition, the critical size for glass formation is rather low.

Several crystalline phases can be distinguished from backscattered SEM images of the Mg51 master alloy (Fig. 2a). The microstructure of the cone slices seems to be refined going from bigger to lower diameters (Figs. 2b, 2c, and 2d). Two different crystalline phases (named A and B) are well evidenced in Fig. 2b (slice of 4 mm diameter) and Fig. 2c (slice of 3 mm diameter). The presence of the same two phases in the various portion of the ingot cast with different quenching rate was inferred from the XRD patterns, where the same diffraction peaks are found for all the slices of the bulk samples, even if a conclusive identification was not possible. The phase identification in this system is quite difficult, due to the high number of elements and to the lack of information in literature on ternary phases in the system Mg-Cu-Y or on higher order phases [13].

Mg51 samples present DSC traces with an evident glass transition temperature (T_g) only for the ribbon (T_g = 175 °C) and for the BMG slices with the smallest diameter (1 mm; T_g = 180 °C), as shown in Fig. 3, curves c and d. The crystallisation behaviour changes progressively, increasing the

Table 1. Thermal properties determined using DSC at a heating rate of 40 °C/min. T_g = glass transition temperature; T_x = crystallisation temperature; $\Delta T_x = T_x - T_g$; $T_{rg} = T_g/T_m$; $\Upsilon = T_x/(T_g+T_l)$; $\Delta T_x = T_x - T_g$; T_m = melting temperature; T_l = liquidus temperature. (T_g, T_x, T_m, T_l, ΔT_x in °C; *Hv* in GPa).

	T_g	T_x	ΔT_x	T_m [a]	T_l [a]	T_{gr}	T_g/T_l	Υ	*Hv*
Mg51 ribbon	175	247	72	416	580	0.65	0.53	0.40	3.10 ± 0.21
Mg51 slices	180	225	45	416	580	0.66	0.53	0.38	3.53 ± 0.19
Mg60 ribbon	165	227	62	416	490	0.63	0.57	0.42	2.84 ± 0.10
Mg60 slices	165	231	66	416	490	0.63	0.57	0.42	2.83 ± 0.15

[a] Melting and liquidus temperatures were measured on master alloys.

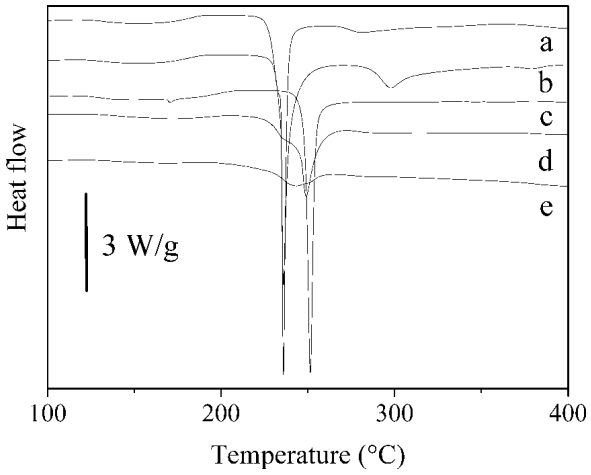

Fig. 3. DSC traces of: (a) Mg60 alloy, cone slices of 4 mm diameter; (b) Mg60 alloy, as quenched ribbon; (c) Mg51 alloy, as quenched ribbon; (d) Mg51 alloy, cone slices of 1 mm diameter; (e) Mg51 alloy, cone slices of 4 mm diameter. The heating rate was 40 °C/min.

crystalline fraction in the alloy, as evidenced in the DSC traces reported in Fig. 3 (curves c, d, and e). A single crystallisation peak is evident for the fully amorphous ribbons (Fig. 3c), with an onset temperature of 247 °C. A shoulder appears, on the low temperature side of the DSC peak, when a sample with crystals embedded in the amorphous matrix is examined, i.e. ingot slice of 1 mm diameter (Fig. 3d). The intensity of the DSC peak decreases more and more, increasing the crystalline fraction and, finally, it disappears when ingot slices of 4 mm are examined (Fig. 3e).

$Mg_{60}Ni_9Cu_9Zn_5Y_6Ag_5Gd_6$

For the Mg60 composition, all samples (ribbons and ingot slices of increasing diameter) were found fully amorphous to XRD. As an example, the XRD pattern of a cone slice of 4 mm (the maximum diameter produced) is reported in Fig. 1, curve b. Therefore, the critical size for glass formation for this composition can be assumed to be at least 4 mm.

Mg60 amorphous samples (ribbons and BMG) present DSC traces with three crystallisation peaks, as shown in Fig. 3 curve a and b, respectively. The T_g is evident at 165 °C for both samples, but the crystallisation temperature is slightly different, i.e. 227 °C for ribbon and 231 °C for cone slices samples.

Melting behaviour for $Mg_{51}Ni_{11}Cu_{13}Zn_4Y_5Ag_7Gd_9$ and $Mg_{60}Ni_9Cu_9Zn_5Y_6Ag_5Gd_6$ master alloys

The Mg51 and Mg60 alloys display similar behaviour during melting, showing the same melting temperature (T_m = 416 °C), but different liquidus temperature (580 °C for Mg51 and 490 °C for Mg60). A similar melting temperature was reported in literature for $Mg_{65}Ni_{7.5}Cu_{7.5}Zn_5Y_5Ag_5Gd_5$ alloy (412 °C [12]), but in that case the liquidus temperature was reported to be 446 °C.

These results seem to indicate that the composition characterised by the lower liquidus temperature for this multicomponent system is close to $Mg_{65}Ni_{7.5}Cu_{7.5}Zn_5Y_5Ag_5Gd_5$ and a decrease of the Mg content in the alloy produces an increase of this temperature. The presence of intermetallic phases with a high melting temperature reduces the GFA of the Mg51 alloy, probably because of their high nucleation tendency during quenching. As a consequence, an increase of the critical cooling rate for glass formation and a related decrease of the critical size is observed and the alloy can be produced completely amorphous only in ribbon form.

All the calorimetric data are collected in Table 1, together with the parameters usually considered for the evaluation of the GFA i.e. T_{rg}, T_g/T_l, Υ and ΔT_x (with $T_{rg}=T_g/T_m$; $\Upsilon=T_x/(T_g+T_l)$; $\Delta T_x=T_x-T_g$), which may explain the observed results on glass formation.

Microhardness

In order to characterise the mechanical behaviour, microhardness measurements were performed on ribbons and bulk samples for Mg51 and Mg60 and the obtained values are reported in Table 1. It is reported in literature that the Tabor relation, that correlates microhardness and σ_f ($\sigma_f = 1/3Hv$), is in good agreement with experimental data for Mg based BMG with similar compositions [14]. Therefore this relation was used in this work to estimate the ultimate fracture strength (σ_f) from microhardness values. For Mg60, a microhardness of 2.84 GPa was measured for both ribbons and bulk amorphous samples and, therefore, σ_f was estimated to be close to 947 MPa. Microhardness values measured for Mg51 amorphous ribbons (3.10 GPa) were slightly lower than those obtained for bulk samples (3.53 GPa); so, σ_f was estimated to be close to 1030 MPa for completely amorphous ribbons and 1177 MPa for partially crystalline bulk samples.

These values can be compared with those reported in literature for similar multicomponent alloys [12,14]. A similarity in σ_f values may be observed for the completely amorphous samples (both Mg60 and Mg51 alloys) with respect to $Mg_{65}Cu_{7.5}Ni_{7.5}Ag_5Zn_5Y_5Gd_5$ BMG which shows a σ_f equal to 928 MPa [12]. When partially crystalline samples are considered (Mg51 bulk samples with estimated σ_f of 1177 MPa), the values of σ_f estimated in this work are similar to those reported for $Mg_{65}Cu_{7.5}Ni_{7.5}Ag_5Zn_5Y_{10}$ with 20% TiB_2 particles dispersed in the amorphous samples (1212 MPa). This analogy seems to indicate that the presence of crystals dispersed in the amorphous matrix may improve the ultimate fracture strength of Mg-based multicomponent alloys.

4. CONCLUSIONS

Glass formation and hardness of two multicomponent Mg-based alloys ($Mg_{51}Ni_{11}Cu_{13}Zn_4Y_5Ag_7Gd_9$; $Mg_{60}Ni_9Cu_9Zn_5Y_6Ag_5Gd_6$) were considered. $Mg_{51}Ni_{11}Cu_{13}Zn_4Y_5Ag_7Gd_9$ alloy is characterised by an higher liquidus temperature with respect to $Mg_{60}Ni_9Cu_9Zn_5Y_6Ag_5Gd_6$. An higher critical cooling rate for glass formation allows the formation of a fully amorphous samples only in ribbon form for $Mg_{51}Ni_{11}Cu_{13}Zn_4Y_5Ag_7Gd_9$ alloy. En estimation of ultimate fracture strength was derived from Vickers hardness ($\sigma_f = 1/3Hv$) and the highest value (σ_f =1177 MPa) was observed for partially crystallised Mg51 BMG.

ACKNOWLEDGEMENTS

Work performed within Bando Regionale Ricerca Scientifica Applicata 2004, progetto D23, Regione Piemonte; MCRTN-CT-2003-504692; MIUR-PRIN 2005-097983-002.

REFERENCES

[1] M.F.Ashby and A.L.Greer // *Scripta Mat.* **54** (2006) 321.
[2] J.Schroers and W.L.Johnson // *Phys. Rev. Lett.* **93** (2004) 255506.
[3] A.Inoue, B.L.Shen and C.T.Chang // *Intermetallics* **14** (2006) 936.
[4] Q.Zheng, S.Cheng, J.H.Strader, E.Ma and J.Xu // *Scripta Mater.* **56** (2007) 161.
[5] F.Guo, S.J. Poon, X.Gub and G.J.Shiflet // *Scripta Mat.* **56** (2007) 689.
[6] L.J.Huang, G.Y.Liang, Z.B.Sun and Y.F.Zhou // *J. Alloy Compd.* **432** (2007) 172.
[7] A.Inoue, T.Nakamura, N.Nishiyama and T.Masumoto // *Mat. Trans. JIM* **33** (1992) 937.
[8] H.Men and D.H.Kim // *J.Mater. Res.* **18** (2003) 1502.
[9] D.G.Pan, W.Y.Liu, H.F.Zhang, A.M.Wang and Z.Q.Hu // *J. Alloy Compd.* **438** (2007) 142.
[10] H.Ma, L.L.Shi, J.Xu, Y.Li and E.Ma // *Appl Phys Lett* **87** (2005) 181915.
[11] H.Ma, E.Ma and J.Xu // *J.Mater. Res.* **18** (2003) 2288.

[12] E.S.Park and D.H.Kim // *J Mater. Res.* **20** (2005) 1465.
[13] M.Satta, M.Palumbo, P.Rizzi and M.Baricco // *Adv. Eng. Mater.* **6** (2007), in press.
[14] Y.-K.Xu, H.Ma, J.Xu and E.Ma // *Acta Met.* **53** (2005) 1857.